現在も通院加療中である.

2. 考　察

当院初診時，両上肢～背部後半にかけて移動性の疼痛を認めており，西洋医学的検査では有意な所見は認めなかったが，主訴や特徴的な圧痛点を認めていたことから線維筋痛症と診断し加療開始となった．器質的疾患は複数の医療機関で除外されてきており，患者も今後の精査については積極的ではない印象であった．そのため当院では東洋医学的な診察，治療を行うとともに，先ずは問診を重点的に行うこととした．

東洋医学的な考察では疼痛性疾患の病因として「内因」である七情の障害から気鬱，肝気鬱血，「外因」である外邪（風，寒，湿，熱，火，燥）の侵入により瘀血，水滞などが発生すると考えられている．疫学的に特に女性に多いと報告されている本疾患では[4]，瘀血，気鬱の所見を示す症例が多数報告されており，瘀血病態に対する駆瘀血剤による治療をはじめ，柴胡剤，附子剤が用いられる事が多い[5]．本症例においては精神不安，火照り，慢性的な疼痛とともに瘀血に特徴的な小腹急結，同時に胸脇苦満も認め，気鬱傾向も示していた．問診と身体所見から長期にわたる私生活のトラブル，家庭環境の悩みや疼痛など自覚症状に対する不安，また身体症状の増悪に関わらず，周囲の理解や医師との信頼関係が十分に構築できず，強度のストレスの持続により内因の障害が進行したため気鬱傾向となり，瘀血も引き起こし気血水のバランス失調による悪循環が生じたと考えられた．駆瘀血，清熱を目的として処方を選択し一定の症状の軽減を認めたが，特に桃核承気湯は「傷寒論」に「太陽病，熱結膀胱，其人如狂，血自下，下者愈．但少腹急結者，与桃仁承気湯」とあり，長期にわたるストレス環境への暴露により太陽病より病期が進行し蓄血の上衝による心の傷害を生じ，瘀血，如狂状態に至り，特徴的な腹証（少腹急結）を示している状態に対し有効とされている[6]．本症例のような心因性の要素が誘因となり客観的な症状や検査異常に乏しく，多くは不定愁訴と捉えられる傾向のある疾患に対し，疼痛に関わらず改めて全人的な東洋医学的診察による弁証論治を検証することが大切であると考えられた．永田勝太郎先生は線維筋痛症を「生き様の疾患」と表現されているように，現代社会のストレスは一層複雑な構造になってきているため，痛みだけでなく精神的なケアも重要となっていることは明らかである[7]．心身を統合的に捉える心身一如の理論に基づく漢方医学的診断および治療は，本疾患に関わらず今後さらに日常診療において重要となることが考えられる．

【文　献】

1) 藤永洋，高橋宏三，引網宏彰，等：線維筋痛症の証の検討．日東洋医誌 59 別冊号：249，2008
2) Wolfe F, Smythe HA, Yunus MB, et al：The American College of Rheumatology 1990 Criteria for the Classification of Fibromyalgia. Arthritis Rheum 33：160 - 172, 1990
3) 伊藤和憲：線維筋痛症に対する鍼灸治療の現状．医道の日本 736：35 - 42，2005
4) 松本美冨士，前田伸治：線維筋痛症―わが国の疫学像と性差．性差医療 2：1089 - 1094，2005
5) 河野清秀：線維筋痛症は，主に駆瘀血剤で改善する．痛みと漢方 19：55 - 60，2009
6) 高山宏世：桃核承気湯．漢方常用処方解説，三考塾，東京，272 - 273.
7) 佐藤泰昌，成川希，田上慶子，等：漢方治療により QOL の著明な改善を認めた線維筋痛症の 1 例．痛みと漢方 17：60 - 66，2007

※　　※　　※

PAIN AND KAMPO MEDICINE Vol.22 (2012)

A case of fibromyalgia treated with the combination of san'oshashinto and tokakujokito.

Junji Moriya[*1], Jun-ichi Yamakawa[*1], Kenji Takeuchi[*2] and Yoshiharu Motoo[*3]

Abstract: We reported a patient with fibromyalgia successfully treated with Kampo medicines.

Patient was a 42-year-old female who had examinations at some hospitals for several years due to the symptoms of myalgia or althralgia. There was no finding on medical examination.

In our hospital she was diagnosed as fibromyalgia, and further diagnosed as oketsu (symptom caused by the blood stagnation) according to the Kampo diagnosis. By the treatment with tokakujokito, visual analogue scale (VAS) of the pain was improved by 50%.

It was suggested that the therapy based on kampo diagnosis should be effective for the disorders, especially for those based on the lack of mind and body uniqueness (shinshinichinyo).

Key words: fibromyalgia, shinshinichinyo, tokakujokito

[*1] Department of General Medicine, Kanazawa Medical University, Ishikawa, Japan

Offprint requests to: Junji Moriya, Department of General Medicine, Kanazawa Medical University, 1-1 Daigaku, Uchinadamachi, Kahokugun, Isikawa 920-0265, Japan

[*2] Department of Anesthesiology, Fukui Saiseikai Hospital, Fukui, Japan

[*3] Department of Medical Oncology, Kanazawa Medical University, Ishikawa, Japan

※ ※ ※

Forschende Komplementärmedizin
Wissenschaft • Praxis • Perspektiven

Original Article · Originalarbeit

Forsch Komplementmed 2012;19:80–85
DOI: 10.1159/000338516

Published online: April 19, 2012

Temporal Changes in Tongue Color as Criterion for Tongue Diagnosis in Kampo Medicine

Satoshi Yamamoto[a] Yuya Ishikawa[b] Toshiya Nakaguchi[c] Keiko Ogawa-Ochiai[d] Norimichi Tsumura[b] Yuji Kasahara[e] Takao Namiki[e] Yoichi Miyake[f]

[a] Center for Kampo Medicine, School of Medicine, Keio University, Tokyo,
[b] Graduate School of Advanced Integration Science,
[c] Graduate School of Engineering, Chiba University, Chiba,
[d] Clinic of Japanese-Oriental (Kampo) Medicine, Department of Otorhinolaryngology & Head and Neck Surgery, Kanazawa University Hospital, Ishikawa,
[e] Department of Japanese-Oriental (Kampo) Medicine, Graduate School of Medicine,
[f] Research Center for Frontier Medical Engineering, Chiba University, Chiba, Japan

Keywords
Kampo medicine · Tongue diagnosis · Tongue image analysis · Tongue color change

Schlüsselwörter
Kampo Medizin · Zungendiagnose · Zungenbildanalyse · Zungenfarbänderung

Summary
Background: In Kampo medicine (Japanese traditional herbal medicine), the appearance of the tongue contains a lot of useful information for diagnosis. However, an inspection of the tongue is not considered to be important in modern medical diagnosis, since the skills applied in the examination are difficult to understand. Thus, we developed an imaging system and algorithm for quantitative analysis of the tongue to provide the traditional techniques of Kampo with greater objectivity. **Materials and Methods:** Tongue images were taken from 9 healthy subjects for 3 consecutive weeks (5 days/week), 12 times a day, with 300 images taken successively within 30 s each time. Then, the temporal color changes in 30 s, 1 day, and 3 weeks were measured in the device-independent International Commission on Illumination (CIE) 1976 L*a*b* color space. **Results:** The tongue color change in 30 s varied between individuals, and it was mainly classified into 3 patterns. This image acquisition system and valid color management should help all tongue-related research, and the 30-s temporal color change might be an important target for further tongue analysis. **Conclusions:** We were able to acquire tongue images without specular reflection and with valid color reproduction, and the color change in 30 s was found to vary. Tongue color changes have not been mentioned in the classics of Kampo medicine, since they were certainly impossible to discriminate by the naked eye. The change during 30 s is a new finding based on the electronic devices, and together they are expected to become a new criterion for tongue analysis.

Zusammenfassung
Hintergrund: In der Kampo-Medizin (japanische traditionelle Kräutermedizin) werden der Zungenbeschaffenheit viele nützliche Informationen zur Diagnosefindung zugeschrieben. Die Beurteilung der Zunge findet sich weniger in der westlichen Medizin, da die Methode als schwierig und die Beurteilung der Zunge als subjektiv gilt. Um der traditionellen Technik der Kampo-Medizin größere Objektivität zu verleihen, haben wir ein bildgebendes Verfahren und einen Algorithmus entwickelt, die eine quantitative Analyse der Zunge erlauben. **Material und Methoden:** An 9 gesunden Probanden wurden in 3 aufeinanderfolgenden Wochen (5 Tage pro Woche) 12-mal täglich Aufnahmen der Zungenoberfläche angefertigt. Während jeder Sitzung erfolgten 300 Aufnahmen innerhalb eines Zeitraumes von 30 s. Die Farbveränderungen innerhalb 30 s, 1 Tages und 3 Wochen wurden dann im geräteunabhängigen International Commission on Illumination (CIE) 1976 L*a*b*-Farbraum gemessen. **Ergebnisse:** Die Farbveränderung innerhalb von 30 s variierte zwischen Individuen und konnte in 3 Hauptmuster unterteilt werden. Die Aufnahmemethode und die zulässige Farbklassifikation sollten in zukünftigen Studien zur Zungenoberfläche nützlich sein. Die Farbveränderung in 30-s-Intervallen könnte ein wichtiges Forschungsobjekt sein. **Schlussfolgerungen:** Es gelang uns, Zungenaufnahmen ohne störende Lichtreflexe und mit verlässlicher Farbwiedergabe aufzuzeichnen. Wir konnten dokumentieren, dass die Farbveränderungen innerhalb 30 s interindividuell variieren. In der klassischen Kampo-Lehre wurden Farbveränderungen der Zunge nicht erwähnt, sicherlich weil sie sich der Beurteilung mit bloßem Auge entziehen. Wir erwarten, dass sich das neue elektronische Verfahren der Bildgebung und der Dokumentation als ein diagnostisch wertvolles Kriterium der Zungenbeurteilung etabliert.

KARGER
Fax +49 761 4 52 07 14
Information@Karger.de
www.karger.com

1661-4119/12/0192-0080$38.00/0

Accessible online at:
www.karger.com/fok

Satoshi Yamamoto
Center for Kampo Medicine
School of Medicine, Keio University
35 Shinanomachi, Shinjuku, Tokyo 160-8582, Japan
Tel. +81 3 5366-3824, Fax -3825
may-s@umin.net

Introduction

In Japanese traditional herbal medicine (Kampo medicine), the appearance of tongue and face, mainly in terms of color, contains a lot of useful information for diagnosis and is an essential factor in visual examination [1, 2]. By assessing the patient's tongue complexion, for example, we are able to assess the degree of mental stress, anemia, and the Oketsu status (blood stagnation: one of the important pathological criteria in Kampo medicine). However, inspection of tongue and face is not considered to be important in modern medical diagnosis, since the skills applied in the examination are difficult to understand and since it does not provide much objective information.

Kampo medicine contains a lot of concepts useful for preventive medicine. For example, 'Mibyou' (disease-oriented state: not a disease, but can easily become one if no cure is applied; contains Oketsu status) is one of the most important concepts for preserving health and preventing illnesses from developing by the early recognition of signs of abnormalities and their treatment. Thus, it can also be useful for modern preventive medicine, but these concepts are nevertheless difficult to disseminate widely since the skills in the diagnosis of Kampo medicine have been thought to require great experience in the traditional examination, such as tongue inspection, pulse diagnosis and/or abdominal palpation, and it is thought that nothing can substitute for experience. Thus, the development of a useful imaging system and an algorithm for a quantitative analysis of the tongue has been eagerly awaited, as it is impossible to have all physicians learn the tongue inspection skills.

Up to now, tongue diagnosis in traditional Chinese Medicine (TCM) has been performed in various ways [3–6]. By these methods, tongue images were clearly classified into known symptoms, but the database was created according to the empirical diagnostic methods of TCM. In terms of only TCM, the algorithms of these methods are very useful, but as they do not focus on physiological properties of the tongue itself, we propose a system for acquiring optically valid color information free from subjective inspection, as well as temporal changes in tongue color as the new criterion for tongue analysis.

Furthermore, some analyses have been focusing on tongue color, but little research has focused on the validation of image acquisition and the effect of specular reflection, which interferes with valid color acquisition. Additionally, for analyzing tongue color, hyperspectral imaging systems were previously developed [7–11]. In these studies, tongue color was acquired in greater detail, but the systems were very expensive, discouraging their common application.

In this article, we propose a tongue image acquisition system with a 3-band camera and an integrating sphere, an algorithm for valid color management, and temporal changes in tongue color as a new criterion for tongue diagnosis. With this system, we are able to acquire images without specular reflection and with valid color reproduction, and it can be expected to prove useful for future studies of the tongue.

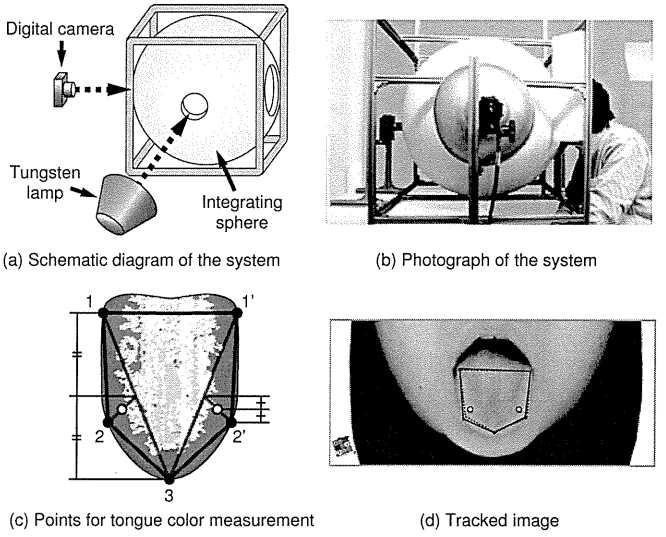

Fig. 1. Imaging system for the tongue and measurement geometry. (**a**) Schematic diagram of the system. (**b**) Photograph of the system. The PC-controlled digital camera, the tungsten lamp, and the integrating sphere are shown. (**c**) Manually selected points and measurement points are shown; the black points are manually selected points, and the white points are measured points; 1, 1': crossing point between lip and tongue edge, 2, 2': tongue edge where the tangent is parallel to the 1–3 or the 1'–3 line, 3: tongue apex. Red points were determined as the center of the segment, which is the center of the 1–3 segment to point 2. (**d**) Tracked image after 10 s; dashed line: manually selected lines as in (**c**), solid line: tracked line for this picture, white points: measured points. Note that in the left-bottom part of (**d**), CasMatch is automatically recognized and image acquisition stability is validated during a series of image acquisitions.

Material and Methods

Imaging System

The imaging system is illustrated in figure 1a, b. A tungsten lamp PRF-300W (Iwasaki Electric Co., Ltd., Tokyo, Japan) was utilized as light source. The integrating sphere (60 cm in diameter, painted matte white with identical reflectance at 400–800 nm) provided diffuse illumination to eliminate artifacts from specular reflections. The stability of the light source was validated by spectrophotometer and oscilloscope. The spectral property shifted to a lower temperature when switched on, stabilized in 10 min, and images were then taken. The luminance of the light source oscillated slightly at a frequency of 100 Hz because of the 50-Hz alternative current power supply. To avoid any influence of this oscillation, the exposure time was set in multiples of 10 ms, because at 100 Hz oscillation, every cycle comes every 10 ms and thus the integral of luminance is the same for all 10 ms. In this experiment, we set the exposure time at 20 ms, which showed the best dynamic range under our conditions.

The digital camera Lu175C (Lumenera Corp., Ottawa, ON, Canada) was used for data collection. This camera features a 10-bit/channel 3-color, red, green, and blue (RGB) CMOS sensor and is capable of taking 30 raw images per second with a resolution of 1280 × 1024 under the control of a personal computer (PC). The subject's face was fixed with a chin rest and a forehead rest. As the mouth cannot be opened when both

Table 1. Tongue color change in 1 day; average, standard deviation and calculated p value of a* among 3 time points: morning (8:30), noon (12:30), and early evening (16:00)

Subject	Respective values			p Value
	8:30	12:30	16:00	
1	26.9 ± 3.0	26.9 ± 2.8	28.1 ± 2.1	0.13
2	35.3 ± 1.6	34.9 ± 1.5	34.8 ± 1.9	0.47
3	34.3 ± 2.3	33.5 ± 2.8	34.6 ± 3.1	0.15
4	30.5 ± 1.9	28.6 ± 2.0	29.8 ± 2.2	0.003**
5	32.3 ± 2.0	31.4 ± 2.1	32.0 ± 2.3	0.22
6	35.6 ± 3.1	35.5 ± 3.3	36.0 ± 2.6	0.83
7	31.0 ± 1.6	30.2 ± 1.9	29.7 ± 1.4	0.04*
8	30.2 ± 4.5	28.7 ± 3.8	30.6 ± 3.1	0.24
9	35.0 ± 2.1	33.8 ± 2.3	35.3 ± 2.4	0.09

*p < 0.05, **p < 0.01.

chin and forehead are fixed, first the chin was placed on the chin rest, the mouth was opened and the tongue was extended, and then the forehead was placed against the forehead rest.

Subjects and Image Acquisition

Images were acquired from 9 healthy Japanese subjects aged 23–25 years (3 men and 6 women) in 3 consecutive weeks, Monday to Friday. Their diet including tea or coffee, habits such as alcohol use and smoking, and daily activities were surveyed by daily interview sheets, and the subjects' tongues, pulse rates and abdomens were examined once a day by a Kampo physician according to the 4 examination methods of Kampo medicine [2]. Almost no changes were observed during these periods according to the Kampo examinations. Images were taken 12 times a day, 4 times at 8:30 in the morning, 4 times at 12:30 before lunch, and 4 times at 16:00. Each tongue extension was for 30 s, and images were taken every 100 ms; in total, 300 images were taken each time. For further color validation, 2 small color charts (CasMatch; BEAR Medic Corp., Tokyo, Japan) were included in the image field. This study was approved by the Ethics Committee of the Graduate School of Medicine, Chiba University, and complies with the Helsinki Declaration.

Calibration and Color Space Conversion

To accurately measure tongue color, tongue images were converted to device-independent color space. The conversion matrix from the RGB color space to the XYZ color space was calculated before image acquisition, as the acquired RGB values are dependent on the light source, the RGB color filter of the camera, and the CMOS sensor, where small changes are observed according to daily conditions such as temperature and humidity. First, a Munsell color chart ColorChecker® Mini (X-Rite Inc., Grand Rapids, MI, USA) was added to the system, and the matrix was constructed by multiple linear regression analysis among the RGB values of respective color patches and their known XYZ values. Then, the acquired images were converted into the device-independent XYZ color space as the product of the computed conversion matrix and the RGB value of each pixel.

The subsequent processes, dependent on visual sense, were performed with XYZ images, because X, Y, and Z emulate the sensitivity of each type of cone cell on the retina, thus appearing natural when shown as R, G, and B, respectively, on the monitor.

Finally, the XYZ color space was converted into the International Commission on Illumination (CIE) 1976 L*a*b* color space, as a* and b* are the opponent color axes and simulate well the color recognition in the visual association cortex; a* is the green-red axis, and b* is the blue-yellow axis. L* is lightness.

Table 2. Details of subjects 4 and 7; calculated p value of a* between each 2 of the 3 time points: morning (8:30), noon (12:30), and early evening (16:00)

Subject	p Value		
	8:30–12:30	8:30–16:00	12:30–16:00
4	0.0004**	0.26	0.03*
7	0.09	0.008**	0.41

*p < 0.05, **p < 0.01.

Tongue Tracking and Color Measurement

As the tongue changes its morphology with time, tongue motion was tracked and the same position of the tongue was analyzed. 5 points were manually selected for the first image as a pentagonal shape to cover the tongue shape, and tongue motion was tracked by the method of Lucas and Kanade [12], which is included in the Open Source Computer Vision (OpenCV) library. Tongue color measurement points were set while avoiding tongue coating, which is easily affected by staining from, e.g., colored foods or coffee. The tongue tip is also avoided because the tip color is easily affected by mental stress. These points were geometrically determined as the part where tongue coating is not observed empirically and color is relatively stable for tongue motion. The selected points and geometrical criteria are shown in figure 1c, d. We extracted 10 × 10 pixels for each point, and the averages of these 200 pixels were subjected to analysis. Both points showed no significant difference in our preliminary experiment.

Measurement Items and Significance Test

Time-related tongue color change was measured for 3 different time spans: (1) 30 s, (2) 1 day, and (3) 3 weeks.

Tongue color change in 30 s: As described under Subjects and Image Acquisition, 300 images were taken at one time. We selected the last day of the 3-week period when the subjects had become accustomed to extending their tongues for 30 s. All images from that day were averaged on a frame-to-frame basis and classified manually. Color change in 30 s was denoted as the difference between the first 3 s (images 1–29) and the last 3 s (images 271–300).

Tongue color change in 1 day: As described above, series of images were taken 12 times a day, 4 times each in the morning, at noon, and in the evening. For this experiment, the first image from each set of 300 images was used in order to eliminate the change in 30 s. Then all values – each of the morning values of 3 weeks, noon values of 3 weeks, and evening values of 3 weeks – were collected for the respective subjects. Color change in 1 day, among 3 time points, was statistically evaluated by 1-way analysis of variance, and between each 2 of 3 time points, evaluation was by Welch's *t*-test.

Tongue color change in 3 weeks: Tongue images were taken for 3 consecutive weeks, Monday to Friday. At first, 4 images – the 1st, 100th, 200th, and 300th images taken at 0, 10, 20, and 30 s after tongue extension, respectively – were picked from each series and averaged to represent each series. Then, the morning, noon, and evening values were averaged with respect to each subject and each day. Finally, 45 values were calculated for each subject. Color change in 3 weeks was statistically evaluated by Welch's *t*-test between the first 7 days and the last 7 days.

Significance test: Significance of difference between 2 groups was evaluated statistically by Welch's *t*-test [13] with a significance level of 5%, for each of the values L*, a*, and b*. In this study, 2-sided hypothesis tests were performed, as we were not able to predict how the color would change. For the tongue color change in 30 s, the significance of the color change was evaluated against the initial pictures. For the color change in 1 day, the significance of difference among the 3 groups was evaluated statistically by 1-way analysis of variance [13] with a significance level of

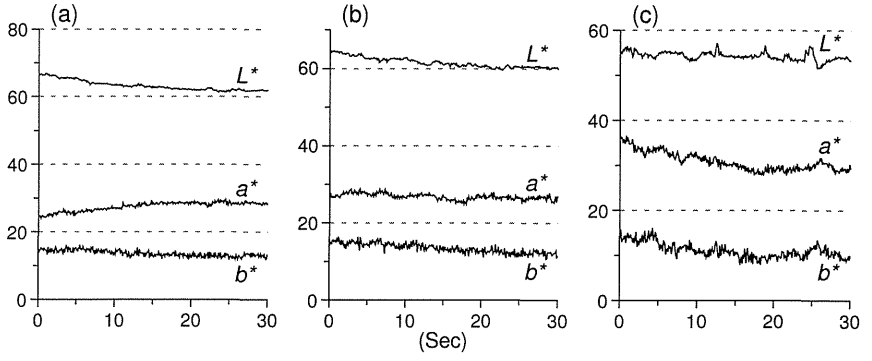

Fig. 2. Tongue color change in 30 s (typical examples). The tongue color change is plotted with L*, a*, and b*, separately. Color change was classified into 3 types by the differences in the changes in a*; (**a**) increasing a* type, (**b**) stable a* type, (**c**) decreasing a* type. Note that L* and b* decrease in all subjects, but the degree of decrease varies among the samples. For L*, a*, and b*, no unit of quantity is required. These changes could not be determined by the naked eye, as the change in color difference in 30 s has a value of 10 (no unit of quantity required) at maximum.

Table 3. Difference between first and last 3 s; average and standard deviation of the a* value of the first 3 s (0–3 s), the last 3 s (27–30 s), and the incremental value

Subject	0–3 s	27–30 s	Increment
1	27.3 ± 0.6	26.4 ± 0.6	–0.9
2	25.0 ± 0.6	28.6 ± 0.3	3.5
3	28.4 ± 0.4	28.5 ± 0.2	0.2
4	34.7 ± 1.1	29.2 ± 0.6	–5.4
5	30.6 ± 0.4	27.4 ± 0.6	–3.1
6	37.8 ± 1.3	29.1 ± 1.0	–8.8
7	33.7 ± 0.7	29.3 ± 0.8	–4.4
8	32.0 ± 0.9	27.7 ± 0.4	–4.2
9	33.4 ± 0.5	29.1 ± 0.6	–4.4

5%, and the average values, standard deviation, and p values are shown in table 1. For subjects showing significant differences among the 3 time points, the differences between each 2 of the 3 time points were evaluated by Welch's *t*-test (table 2).

Results

Tongue Color Change in 30 s

In all subjects, L* (lightness) and b* (blue-yellow axis) decreased. In other words, the tongue color got darker and pale in all subjects, possibly caused by decreasing blood flow due to the tongue extension. Also a* (green-red axis) decreased in most subjects. However, some subjects showed stable or increasing a*. The maximum increase was approximately by an increment of 3, and the maximum decrease was approximately 10 (table 3). For future experiments and data collection, we set cut-off values at 3 and classified into 3 types – decreasing a* type (subjects 4, 5, 6, 7, 8, and 9), increasing a* type (subject 2), and stable a* type (subjects 1 and 3). Typical examples are shown in figure 2. By mere observation, these changes could not be detected as the change of the color difference in 30 s was too small; a value of approximately 10 (no unit of quantity required) at maximum is necessary to be discernible by the naked eye.

Tongue Color Change in 1 Day

In this experiment, a* varied more than L* and b* among subjects or in the same subject; therefore, the results of the analysis of a* are shown in table 1. The subjects showing a significant difference by 1-way analysis of variance (subjects 4 and 7) were further inspected between each 2 of the 3 time points by Welch's *t*-test, as shown in table 2. In subject 4, the color at noon was significantly different, and in subject 7 in the evening, but in the other 7 subjects there were no significant changes in 1 day. Suspecting that this phenomenon was due to common daily activities, such as teatime and alcohol consumption, the daily interview sheets were analyzed and additional interviews were performed, but no particular habits were revealed. On average, color difference has a value of approximately 2 (no unit of quantity required), and differences may be determined by a color expert under suitable conditions using comparisons; they cannot be determined by tongue inspection without comparisons.

Tongue Color Change in 3 Weeks

The changes during 3 weeks are shown in figure 3. No statistical and characteristic changes were observed in any of the subjects. Subject 9 had an 8-day span during this period because of catching a cold, but no significant change was observed between before and after this span.

Discussion and Conclusion

The color of the tongue presents a lot of useful information for medical diagnosis. In spite of this, research centering on valid tongue imaging, which would assist the study of tongue color, has been very limited. For tongue color analysis, specular reflection should be completely eliminated, as it contains only information of the light source, not of the tongue. There are many methods to eliminate specular reflection; in a preliminary experiment we tried 3 methods, a multiple light source, a polarizer, and an integrating sphere. With the multiple light source, illumination was with all sources at 45° to the tongue; however, by this method, elimination of specular reflection

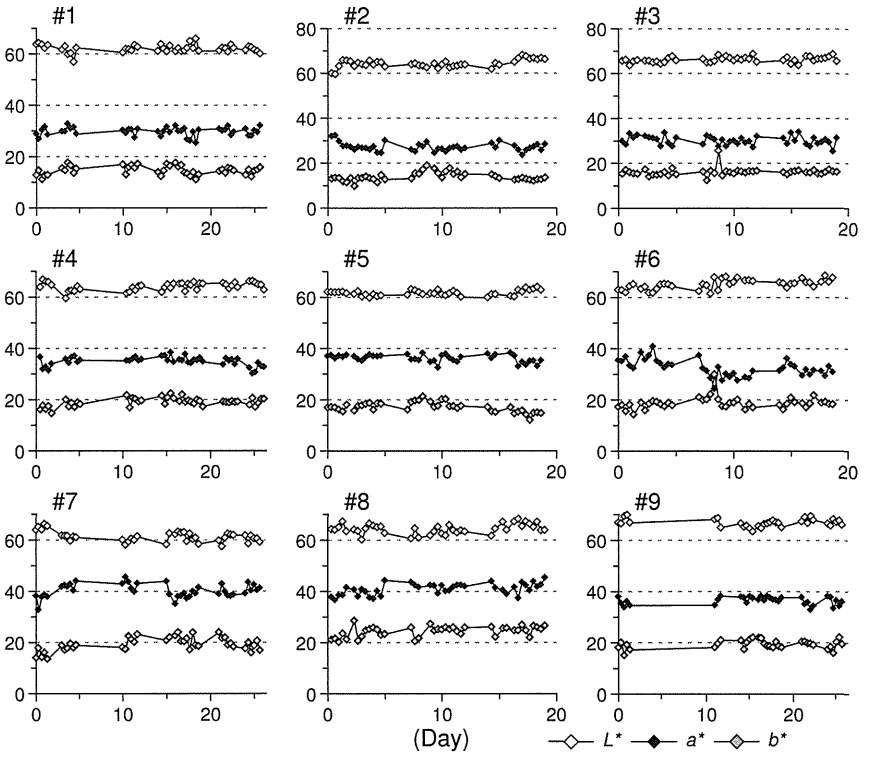

Fig. 3. Tongue color change in 3 weeks. Total days vary because of holidays. Numbers are for identification and are the same numbers as in table 1. Subject 9 suffered from a cold from day 2 to 9, so points are lacking in this interval. For L*, a*, and b*, no unit of quantity is required.

was incomplete. Then, we set 2 polarizers orthogonally in front of the camera and the light source; reflection elimination was perfect, but luminance was insufficient for continuous shooting. Finally, the integrating sphere supplied diffuse light, specular reflection was completely removed, and luminance was high enough for continuous shooting, leading us to select this method. However, the integrating sphere requires larger material than the other two methods, namely, a 60-cm diameter ball. We employed this size for whole-face imaging, and a smaller system is suitable for tongue analysis only. We have already prepared a system with a 30-cm integrating sphere for additional data acquisition, and its accuracy was validated.

Tongue area extraction and segmentation have been previously performed by Zhang et al. [14]. In their methods, the tongue could be extracted clearly, although elimination of the coating was incomplete. We tried the snake method, which is an active contour method, to find the contour by minimizing its energy dependency on the contrast of the border, with the same algorithm [14], but our image showed poor results, despite good results in terms of specular containment. This algorithm was dependent on specular reflection and shadow, which enhances the contrast of the tongue edge. Thus, for this study, we selected the tongue portion manually, and tongue motion was tracked automatically by the method of Lucas and Kanade [12]. Still, tongue recognition needs further improvement for automated analysis.

For diagnosis, a tongue color database is frequently employed [3–5, 15]. Although the recognition performance is quite good with these methods, the databases are assembled according to the criteria of TCM, namely, subjective inspection by physicians. On the other hand, our algorithm is not influenced by any subjective issues, but the meaning of tongue color change is still unclear. Valid color information and a tongue database in combination complement each other by lessening the dependence on subjective inspection and describing diseases in algorithms.

Traditional tongue analysis in Kampo classics is the analysis for one moment, i.e., there are many mentionings of momentary tongue color in the classics but few mentionings of tongue color changes over time, because it was impossible to determine the quantitative tongue color change by the naked eye. In this article, we present an imaging system and an image processing method for valid tongue color acquisition, and we analyzed the tongue color change over various time spans. Our system revealed varying changes in tongue color among subjects, which are not mentioned in the classics, and these changes are expected to become a new criterion of tongue analysis. In the first Results section, we showed the tongue color changes in a short time span, 30 s. In all subjects, the tongue color showed a significant temporal change, and the patterns of change were classified into 3 types by the difference in a*. On the other hand, the L* and b* values decreased in all subjects, with the degree of decrease varying among the individuals. Tongue extension can represent artificial blood and water stagnosis as the stress test. The color change in 30 s may represent the degree of stagnation and

staging of 'Oketsu' – a diagnosis of Kampo for blood stagnation, reflecting blood viscosity and aggregation of red blood cells in capillaries; leads to variable symptoms including premenstrual syndrome [1, 2]. Although the origin of this difference is not yet apparent, it may become an important point for diagnostic procedures, as it contains no empirical subjective observation and is easily acquired from outpatients. We are currently collecting more subject data to determine the correlation between this color change and clinical indications, searching for the biomedical phenomenon from which this color change originates, and looking for additional criteria for digitizing the color change curve by such methods as linear approximation and Fourier transformation. As can be seen in the second Results section, in most cases color change was not apparent in 1 day. This means that, in essence, we are allowed to take images whenever we like. While color change may indicate some physiological change, we need further inspection. As seen in the section describing the color changes in 3 weeks, no color change was observed when clinical features did not change. In our experience, tongue appearance changes along with health condition. Therefore, measuring should ideally take place when physiological change is occurring, to identify beneficial color changes of the tongue. Taken together, we are focusing on changes in individual subjects, since such changes have not been reported previously. From another point of view, when focusing on the changes between individuals, the L*a*b* values showed significant differences in our system. We have to collect more subjects, with or without diseases, for further inspection. The proposed system and algorithm properly acquired the tongue color, and the tongue color was found to change in a certain period. Further research regarding the clinical meaning of the findings and differences among individuals is now underway, with larger study populations.

Acknowledgement

This work is a part of the Regional Innovation Cluster Program, City Area Type, by the Ministry of Education, Culture, Sports, Science and Technology.

Disclosure Statement

None of the authors has any conflict of interest to declare in relation to this article.

References

1 Terasawa K: KAMPO: Japanese-Oriental Medicine – Insights from Clinical Cases. Tokyo, KK Standard McIntyre, 1993.
2 The Japan Society for Oriental Medicine: Introduction to Kampo – Japanese Traditional Medicine. Tokyo, Elsevier Japan, 2005.
3 Pang B, Zhang D, Li N, Wang K: Computerized tongue diagnosis based on Bayesian networks. IEEE Trans Biomed Eng 2004;51:1803–1810.
4 Pang B, Zhang D, Wang K: Tongue image analysis for appendicitis diagnosis. Inform Sci 2005;175:160–176.
5 Zhang D, Pang B, Li N, Wang K, Zhang H: Computerized diagnosis from tongue appearance using quantitative feature classification. Am J Chin Med 2005;33:859–866.
6 Wang Y, Yang J, Zhou Y, Wang Y: Region partition and feature matching based color recognition of tongue image. Pattern Recognit Lett 2007;28:11–19.
7 Liu Z, Yan J, Zhang D, Li Q: Automated tongue segmentation in hyperspectral images for medicine. Appl Opt 2007;46:8328–8334.
8 Qing-Li L, Yong-Qi X, Jian-Yu W, Xiao-Qiang Y: Automated tongue segmentation algorithm based on hyperspectral image. J Infrared Millim Waves (Hongwai yu Haomibo Xuebao) 2007;26:77–80 (in Chinese).
9 Zhi L, Zhang D, Yan J, Li Q, Tang Q: Classification of hyperspectral medical tongue images for tongue diagnosis. Comput Med Imaging Graph 2007;31:672–678.
10 Yamamoto S, Tsumura N, Nakaguchi T, Namiki T, Kasahara Y, Terasawa K, Miyake Y: Regional image analysis of the tongue color spectrum. Int J Comput Assist Radiol Surg 2011;6:143–152.
11 Yamamoto S, Tsumura N, Nakaguchi T, Namiki T, Kasahara Y, Ogawa-Ochiai K, Terasawa K, Miyake Y: Principal component vector rotation of the tongue color spectrum to predict 'Mibyou' (disease-oriented state). Int J Comput Assist Radiol Surg 2011;6:209–215.
12 Lucas B, Kanade T: An iterative image registration technique with an application to stereo vision. International Joint Conference on Artificial Intelligence (IJCAI '81) 1981;674–679.
13 Johnson R, Bhattacharyya G: Statistics: Principles and Methods, ed 3. Hoboken, John Wiley & Sons, 1996.
14 Zhang H, Zuo W, Wang K, Zhang D: A snake-based approach to automated segmentation of tongue image using polar edge detector. Int J Imaging Syst Technol 2006;16:103–112.
15 Li Q, Liu Z: Tongue color analysis and discrimination based on hyperspectral images. Comput Med Imaging Graph 2009;33:217–221.

AN ATTEMPT OF EVALUATION ON OIL INSUFFICIENCY IN BALL BEARING WITH ULTRASONIC TECHNIQUE

Akitoshi Takeuchi
Kochi university of technology, Tosayamada-chou Kami-shi Kochi 782-8502 Japan
takeuchi.akitoshi@kochi-tech.ac.jp

Osamu Yokota
Nihon university, Tamura-machi Koriyama-shi Fukusima 963-8642 Japan
yokota@mech.ce.nihon-u.ac.jp

Abstract: The purpose of this study is to evaluate the lubrication condition in ball bearing with the variation of ultrasonic echo height ratio H_{T2} reflected from a contact surface between an outer ring and a ball. When sufficient oil is supplied to the inlet of contact surface between the outer ring and the ball, the echo height ratio which is continued decrease as the ball approaches a sound axis of ultrasonic probe increases locally. However, degree of its increase becomes lower when oil supply is insufficient, and does not appear at all with running out of oil. Moreover, it is cleared that the area of closed curve formed by the relationship between H_{T1} (reflected from the interface of housing and outer ring) and H_{T2} decreases with passage of time, in early stage of operation. However, it is kept with almost constant value in case of insufficient oil supply condition.

Keywords: oil insufficiency, ultrasonic technique, echo height, ball bearing, lubrication condition

1. Introduction

In recent years, amount of lubricant supply to a bearing has been decreased for saving energy of machine, and hazard of the damage in a bearing with sudden deterioration of lubrication conditions under insufficient oil supply is increasing. Therefore, establishment of the method to detect the insufficient oil supply is expected. Lubrication condition of bearing has been usually diagnosed by vibration method, acoustic emission and shock pulse method [1][2]. However, these are diagnostic methods which indirectly estimate the lubrication condition from observed wave form, and are not direct detection methods of the damage and of oil insufficiency.

Ultrasonic technique employed in this study have been used for estimating a lubrication condition and operation abnormalities in ball bearing by the reflection echo height variation from a contact surface between housing and outer ring [3][4][5][6]. Then, it became possible to estimate the width of small and shallow indentation which has a geometry approximately same with a real damage. In addition, estimation of oil film thickness less than 1μm at the center of the elastohydrodynamic lubrication (EHL) region between ball and disc became possible [7][8]. Where, EHL means a hydrodynamic lubrication condition which has an elastic deformation of contact bodies and a sudden increase of viscosity, under extreme pressure.

In this study, the potential on the evaluation of insufficient oil supply by the reflection echo height variation from the contact surfaces of housing, outer ring and ball is investigated.

Then, some simple and convenient indexes for the detection of deterioration of lubrication condition were clarified.

2. Experimental equipment and observation principal

Figure 1 is a schematic view of the experimental equipment. Open type single row deep groove ball bearing (6212) with 70[mm] pitch diameter was used for the oil lubrication test, and experiment was performed under rotating speed of 1000[rpm] and pre load of 40[kN]. Oil insufficiency of the test bearings was examined by using 2[MHz] longitudinal wave probe having a piezoelectric element diameter of 10[mm] attached on the outside of the steel housing. The repetition frequency of the ultrasonic pulse was set to 10[kHz], and data was collected every 100[μs] by an A/D converter. In this experiment, the measurement of vibration and bearing temperature was performed to compare the detectable sensitivity of insufficiency of oil with ultrasonic method. And then, averaged vibration voltage was used only for the evaluation of deleterious change of lubrication condition due to oil insufficiency.

Evaluation principle of insufficient oil supply in a ball bearing using an ultrasonic technique is shown in Figure 2. A part of ultrasonic wave sent from a probe attached on a bearing housing is transmitted to the outer ring of ball bearing through an interface of the outer ring and the bearing housing, and arrives at a boundary surface with a ball. Those interfaces are composed with slight solid contact parts and thin aerial layer when two dried surfaces contacted each other, because there are roughness and waviness on machined surfaces. Therefore, a part of ultrasonic wave sent from ultrasonic probe is reflected in proportion to the solid contact area decided by contact pressure, and the difference of acoustic impedance (included oil film) in ultrasonic irradiation region. And, first reflection echo (height h_1) reflected from the slightly rough machined interface of housing and outer ring, and second reflection echo (height h_2) from the mirror finished rolling surface of outer ring, are observed on the display of flaw detector as shown in Figure 2.

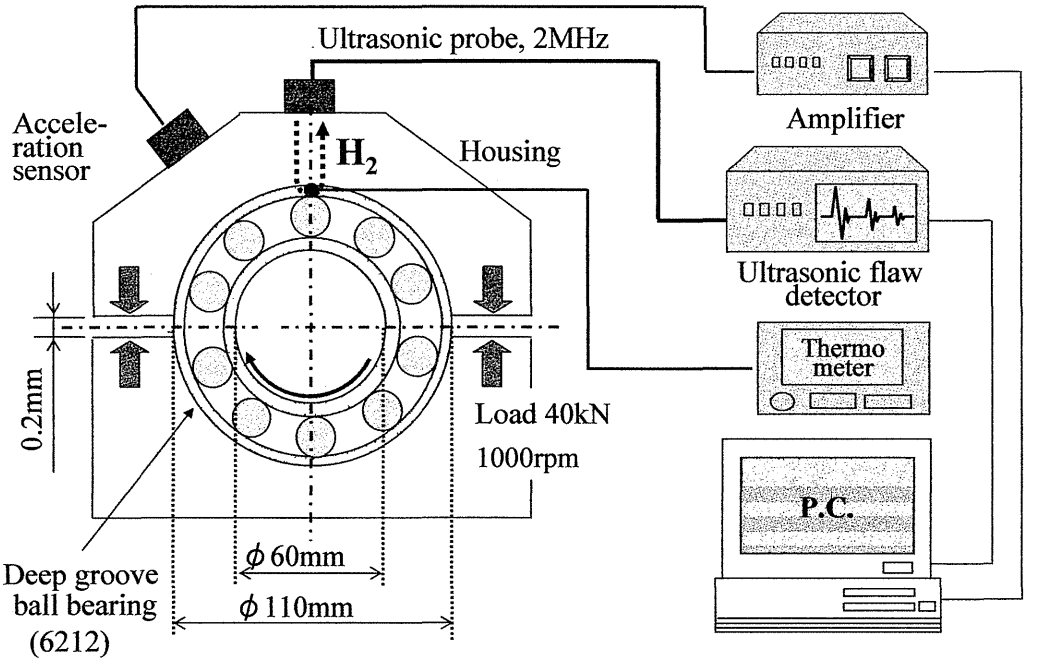

Figure 1 Schematic view of experimental equipment

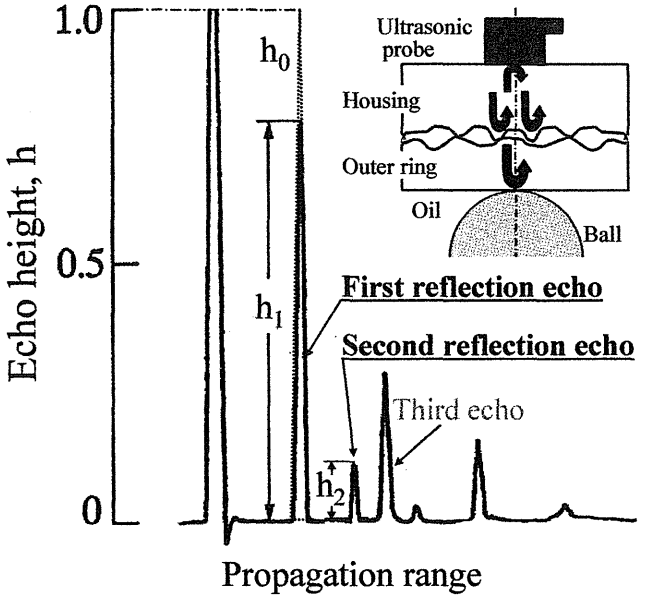

Figure 2 Evaluation principal of insufficient oil supply

These echo height are varied with the characteristic and mounting conditions of the probe, and diffusion and scattering of the ultrasonic wave on propagation path. Then echo height ratio $H_T=(1-h/h_0)\times100$ is employed to evaluate the lubrication condition without these influences. In this equation, h corresponds to h_1 or h_2, and h_0 is the echo height reflected from the interface of housing and outer ring at the ball position that two neighboring balls are equidistant from the sound axis of probe. Therefore the echo height ratio $H_{T1}=(1-h_1/h_0)\times100$ and $H_{T2}=(1-h_2/h_0)\times100$ indicate the transmission ratio of the ultrasonic wave through each interface. Since the echo height h_0 during operation increases and decreases with the variation of contact condition between housing and outer ring, h_0 before the test was set to 0.5.

Supply condition of lubrication oil to the lubricating surface is observed with the second reflection echo height ratio H_{T2}, and the first reflection echo height ratio H_{T1} is used for specifying the ball position and sound axis of ultrasonic beam.

3. Evaluation indexes of oil supply condition

Figure 3 shows the evaluation indexes of oil supply condition. (A), (B), (C) and (D) in Fig. 4(c) are the ball positions as follows. (A): ball is separated enough from sound axis, (B): there is sound axis at the entrance of ball as shown in Figure 4 (b), (C): there is ball on the sound axis as shown in Figure 3 (a), (D): there is sound axis in an exit point of ball.

Transmission of ultrasonic wave from housing to outer ring is increased when a ball supporting load approaches to the sound axis. However, ultrasonic wave arriving at inner surface of outer ring is not transmitted to ball side in case of dry condition shown in Figure 3 (a) or roughening condition, even when ball is on sound axis. On this account, echo height h_2 of reflected wave from inside of outer ring becomes large as ball approaches to sound axis, and echo height ratio H_{T2} decreases as shown by dashed line. Subsequently, H_{T2} increase again as a ball leaves from the sound axis, and it shows a concave in total.

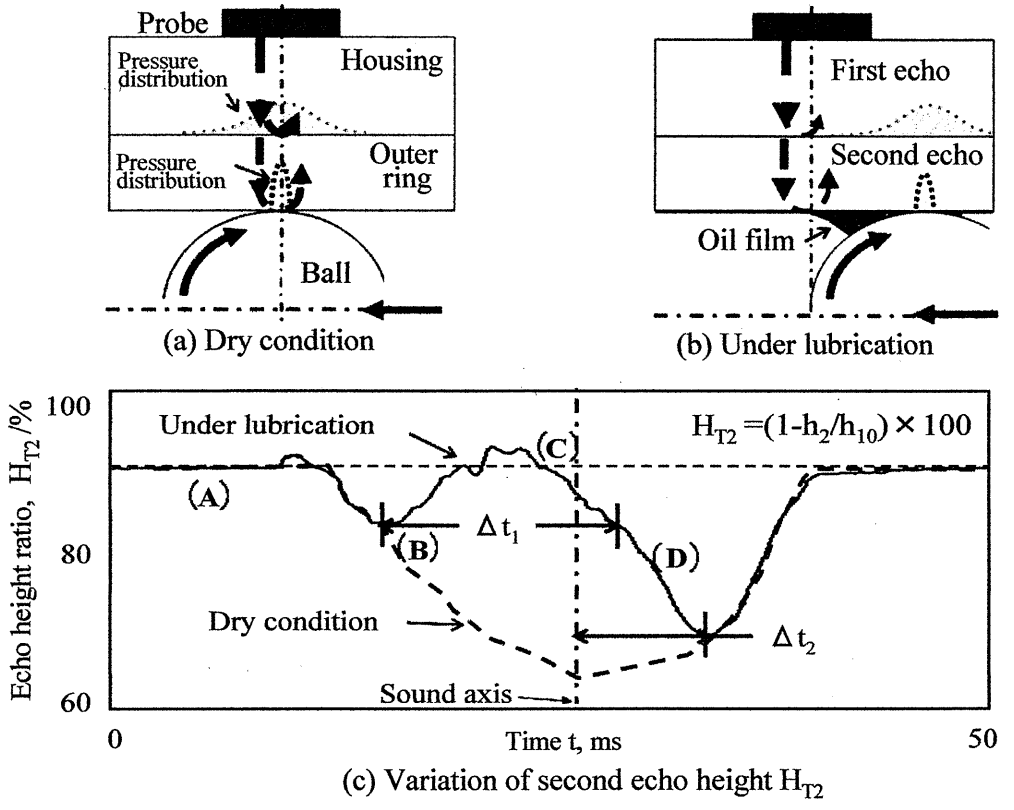

Figure 3 Evaluation indexes of oil supply condition

On the other hand, when sufficient oil is supplied to the inlet of contacting surface, the echo height that continued decrease as the ball approaches to the sound axis of ultrasonic probe is increased locally as shown by Δt_1 in Figure 3 (c) because ultrasonic wave is transmitted to the oil film. The oil film formation region at the inflow side to contribute for transmission of ultrasonic wave is wider than that of exit side, as shown in Figure 3 (b). Then, a peak of convex curve of H_{T2} appears at inflow side of the ball, and H_{T2} reduces up to dashed line which shows dry condition as the inflow side of ball goes away from the sound axis.

Therefore, it is possible to evaluate the condition of oil film formation at inflow side with degree of increment of H_{T2} there. However, the amplitude of H_{T2} is influenced with not only the oil film formation but also the contact condition between housing and outer ring. Since this contact condition varies during operation, h_0 from its interface and h_2 from the interface of outer ring and ball are varied with time, even if oil film formation is the same. Thus amplitude of H_{T2}, $(1-h_2/h_0)\times 100$, is unsuitable for the index of oil insufficiency.

Therefore, duration time Δt_1 that increment of H_{T2} is kept is employed as an index of insufficient oil supply, in this study. Duration time Δt_1 of its increase becomes shorter when oil supply becomes insufficient, and does not appear at all with running out of oil.

A time lag Δt_2 between a bottom of a valley in echo height variation curve and the sound axis of ultrasonic probe is also an effective evaluation index on insufficient oil supply. Δt_2 indicates the degree of differential of oil film formation condition between inflow region and outflow region. And Δt_2 has the potential which can detect the existence of slight oil at inflow region with high sensitivity than that of Δt_1. Hence, it is thought that Δt_2 decreases gradually when oil supply becomes insufficient, and becomes zero with running out of oil at a contact surface.

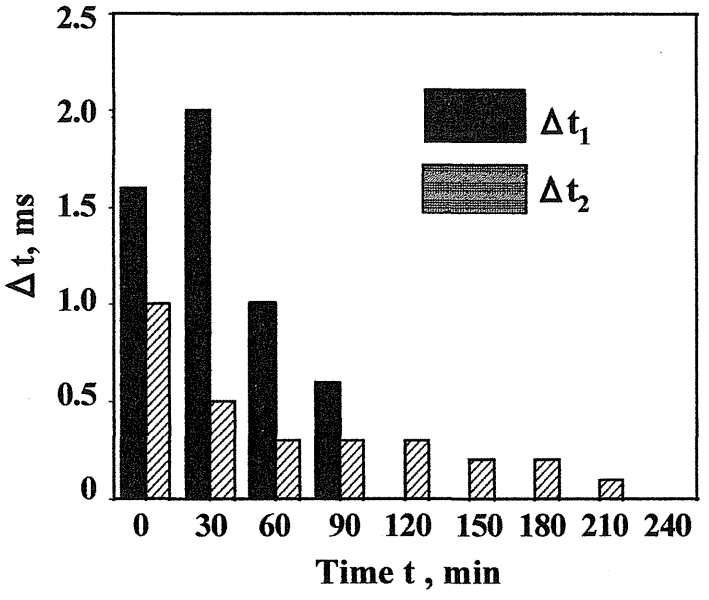

Figure 4 Variation of Δt_1 and Δt_2 measured by ultrasonic method

Figure 4 shows the variation of Δt_1 and Δt_2 measured by ultrasonic method at every 30 minutes, from start-up to 240 minutes. Δt_1 and Δt_2 are decreased gradually with passage of time, in particular Δt_2 which indicates the degree of difference of oil film formation condition between inflow region and outflow region shows continuous change for a long time. Therefore, it is considered that index Δt_2 is effective to evaluate the lubrication condition of ball bearing operated under a trace amount oil supply. And then, it can be estimated that effective oil film was existed at inlet region until 90 minutes, at least. In this way, these indexes are useful to evaluate the lubrication condition including oil insufficiency.

However, it is difficult to detect Δt_1 and Δt_2 in in-situ observation. More convenient method to evaluate the oil insufficiency is necessary for a lubrication diagnosis having hi-reliability. Upper figures in Figure 5 show the typical behavior of H_{T1} and H_{T2} from start-up to 1200min, and lower figures are the relationship between H_{T1} and H_{T2}. H_{T2} is used for the observation of oil insufficiency and the H_{T1} is for specifying the ball position and the sound axis of ultrasonic beam.

In those figures, notation '1' corresponds to the approaching process '1' shown in upper figure, notation '2'corresponds to the hump part of H_{T2}, '3' is the position where boll is on the sound axis, and minimum H_{T2} appeared at point '4' in start-up stage. The shape of those closed curves is varied with accumulation time. For instance, in case of sufficient oil supply condition, H_{T2} has a hump '2' after temporary decreasing, and minimum point '4' of H_{T2} appears in small H_{T1} region. However, such a hump of H_{T2} and minimum point corresponding to '4' do not appear, after passage of 240 minutes. Those closed curves are constantly repeated with passage of the ball if supply conditions of lubricant are the same. Then relationship between H_{T1} and H_{T2} shown by closed curve seems to be a useful index for in-situ observation of the oil supply condition.

However, it is not easy to make sure of a feature of a closed curve corresponding to lubrication condition instantly. Observation of the variation of closed curve area seems to be a useful index for the evaluation of the oil insufficiency rather than making sure of a feature of closed curve, since the area of closed curve decreases with the accumulation time as shown in Figure 5.

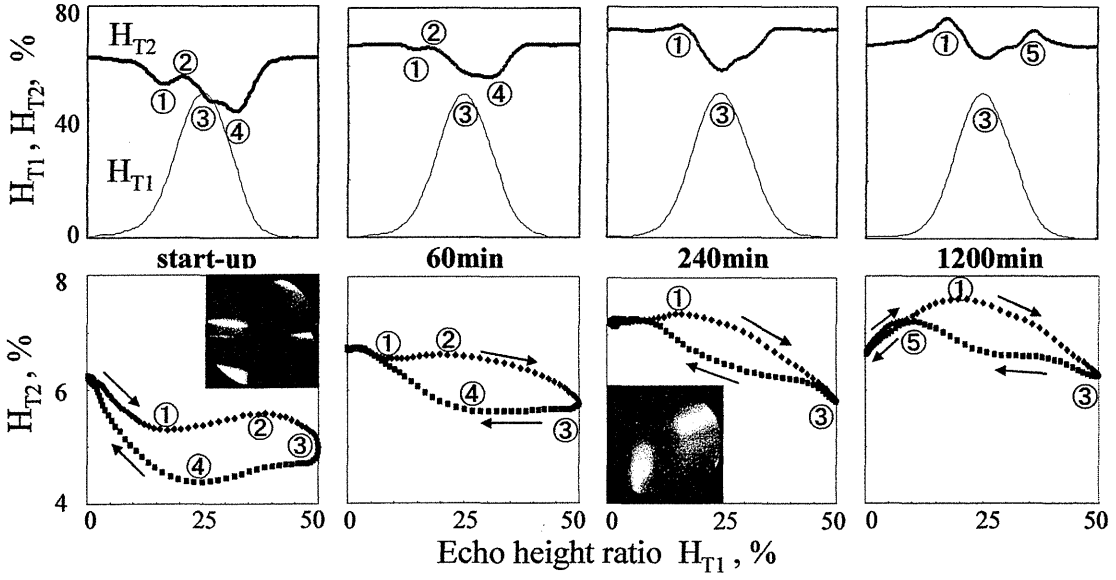

Figure 5 Behaviors of H_{T1}, H_{T2}, and relations between them

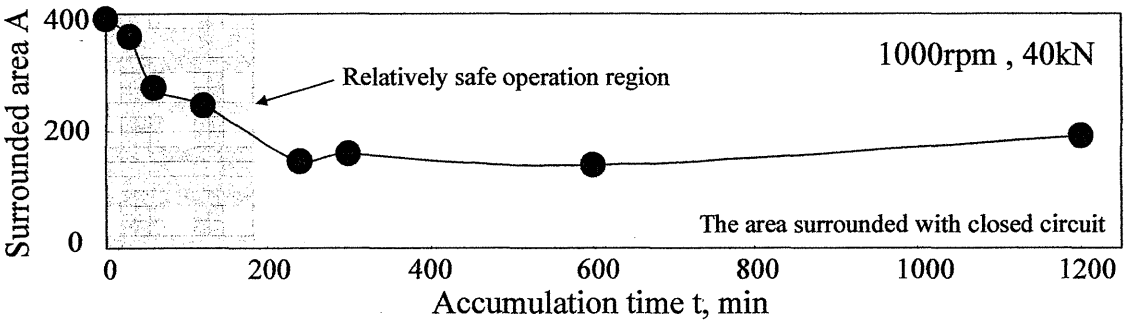

(a) Variation of surrounded area

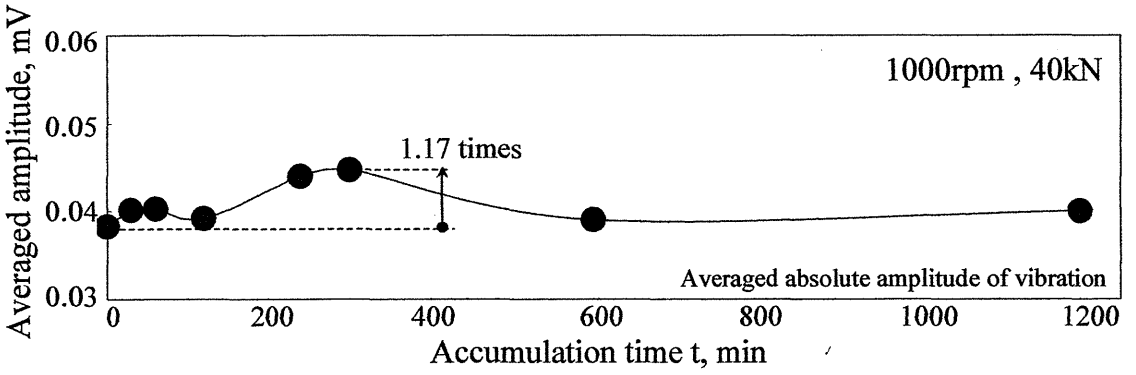

(b) Variation of averaged amplitude of vibration

Figure 6 Variations of surrounded area and average amplitude of vibration

Figure 6 shows the tendency of variation on the area of closed curve. The surrounded area in early stage of operation, from start-up to 240 minutes, is continuously decreased as supply of oil becomes insufficient. However, its area is kept almost constant after passage of 240 minutes because of running out of oil from the contact surface. So it is estimated from some indexes above that effective oil film was supplied until 90 min, in this case at least. In case of vibration shown in Figure 6, the remarkable variation of behavior such as closed curve area cannot be observed even though the vibration is slightly increased, 1.17 times, temporarily near 300 minutes.

4. Conclusions

The potential that is able to evaluate the lubrication condition of ball bearing operating under insufficient oil supply condition was clarified by the observation of behavior of ultrasonic echo height ratio H_{T2} reflected from the interface of ball and outer ring.

1) Oil supply condition at inlet side is shown by Δ_{t1}, and it approaches to zero as supply of oil becomes insufficient.
2) Differential of oil film formation condition between inlet region and outlet region is evaluated by Δ_{t2}, and it decreases in case of insufficient oil supply condition.
3) The area of closed curve formed by the relationship between H_{T1} and H_{T2} decreases with passage of time in early stage of operation. However, it is kept with almost constant value in case of insufficient oil supply condition.

References

[1] T. Yoshioka, S. Shimizu, H. Mano, A. Korenaga, H. Inaba and T. Wakabayashi: Journal of Japanese Society of Tribologists 51-8 (2006) pp. 607-614.
[2] T. Yoshioka and S. Shimizu: Journal of Japanese Society of Tribologists 55-11 (2010) pp. 819-826.
[3] A. Takeuchi: Key Engineering Materials 270(2004) pp. 252-257.
[4] A. Takeuchi, S. Terada and S. Toda: 3rd Asia International Conference on Tribology Kanazawa (2006) pp. 713-714.
[5] A. Takeuchi: Journal of Japanese Society of Tribologists 51-2 (2003) pp. 422-427.
[6] J. Zhang, B. W. Drinkwater and R. S. Dwyer-Joyce: ASME J. Tribol. 128 (2006) pp. 612-618.
[7] R. S. Dwyer-Joyce, B. W. Drinkwater, C. J. Donohoe: Proceedings of the Royal Society London A (2003) pp. 957-976.
[8] A. Takeuchi, S. Terada and S. Toda: International Conference on Advanced Technology in Experimental Mechanics (2007) pp. 42.

STUDY ON SURFACE QUALITY MEASUREMENT OF FLEXIBLE MATERIALS BY AIR JET

Osamu YOKOTA
Department of Mechanical Engineering, College of Engineering Nihon University. 1 Nakakawahara Tokusada Tamura-machi,Koriyama-shi,Fukushima,963-8642, Japan
E-mail:yokota@mech.ce.nihon-u.ac.jp

Kotaro YATABE
Doctor's Course, Mechanical Engineering, Graduate School of Engineering Nihon University. 1 Nakakawahara Tokusada Tamura-machi,Koriyama-shi,Fukushima,963-8642, Japan
E-mail:goblin@mua.biglobe.ne.jp

Mitsuo NAGAO
Department of Mechanical Engineering, College of Engineering Nihon University. 1 Nakakawahara Tokusada Tamura-machi,Koriyama-shi,Fukushima,963-8642, Japan
E-mail:nagao@mech.ce.nihon-u.ac.jp

Akitoshi TAKEUCHI
School of System Engineering,Kochi University of Technology
Tosayamada, Kochi 782-8502 Japan
E-mail:takeuchi.akitoshi@kochi-tech.ac.jp

Abstract: Measuring method for the softness and the viscoelasticity property has not yet been established. The test method which could measure the surface texture of soft objects for processed food and perishable foodstuff is established and the development of the functional equipment is desired. In this study, the dents were made to arise using air jet on the surface of soft object. The shape of the dents is measured in the two-dimensional laser beam. The measuring method of the softness was proposed by the measurement of diameter and depth of the dents which measured soft object. And the method for examining the viscoelasticity property by time course of the dents depth was proposed. The functional testing equipment based on them was manufactured and the soft object was measured. As a result, creep and creep recovery for the depth of the dents were clearly also obtained. Therefore, the measurement of soft object was possible for this measuring method, and it was possible to confirm the performance and the advantage.

Keywords: softness, creep, creep recovery, viscoelasticity, nozzle, laser-aided diagnostics, surface shape measurement

1. Introduction

To the best of our knowledge, there have been few reports on test methods for the viscoelastic properties of soft objects using an air jet instead of plungers for loading and unloading. We propose a method of evaluating their viscoelastic properties, such as soft processed foods and industrial products, using an air jet with newly developed test equipment.

In this method, loading and unloading can be performed using an air jet in a very short time, loading time can be arbitrarily set, and the shape of the dents formed on the surface of soft objects can be instantaneously measured using light from a semiconductor laser. In this study, using the developed equipment, we measured the shape of the dents formed on soft samples, measured the depth of the dents for various loading times, types of soft sample, and pressures, and evaluated the viscoelastic properties of the soft samples with respect to elastic compliance and equivalent dent depth.

2. Creep and Creep Recovery Compliances

Figures 1(a) and 1(b) show the creep and creep recovery curves and the four-element model used to obtain the curves, respectively. Figure 1(a) shows the curve of the creep compliance $J_{(t)}$ when a load is applied at t=0 and that of the creep recovery compliance $J_{r(t)}$ when the load is removed at t=t_r. In the creep phenomenon, the depth of a dent, $h_{(t)}$, increases with time, t, under a constant load F. In the linear viscoelastic creep phenomenon, in which $h_{(t)}$ is proportional to F, $h_{(t)}$ also increases with t under a constant load F. In this case, eq. (1) holds.

$$h_{(t)} = F \cdot J_{(t)} \quad , \quad \therefore \quad J_{(t)} = h_{(t)} / F \tag{1}$$

$J_{(t)}$ in eq. (2) can be divided into three terms as follows.

$$J_{(t)} = J_g + (J_e - J_g) \cdot \Psi_{(t)} + t/\eta \tag{2}$$

Here, J_g is the instantaneous compliance, J_e is the steady-state compliance at t=∞, η is the viscosity coefficient, and $\Psi(t)$ is the creep function, which increases from $\Psi(0)$=0 to $\Psi(\infty)$=1.

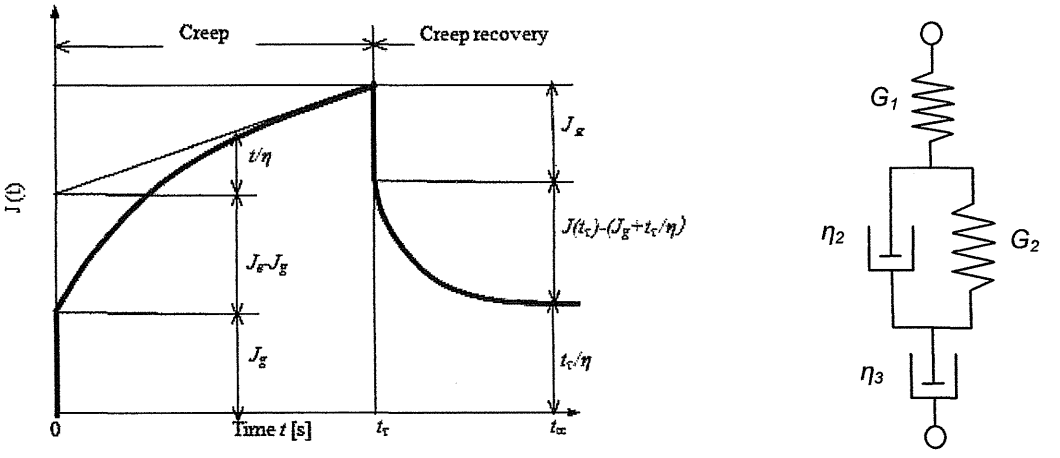

(a) Creep and creep recovery. (b) Four elements equivalent model.

Fig.1 Viscoelasticity property obtained creep and creep recovery.

3. Noncontact Measurement Method for Surface Texture

3.1 Measurement principle

Unlike conventional methods that use plungers for the loading of soft samples, the proposed measurement method uses an air jet with newly developed functional test equipment that can measure the softness and viscoelastic properties of foods and parts of living bodies. As shown in Fig. 2, air is ejected from a nozzle onto the surface of a soft sample. The surface of the soft sample does not deform when exposed to a weak air jet or when the distance between the nozzle and the sample is relatively long; however, it forms a dent when exposed to a strong air jet. Thus, the dimensions of dents are considered to greatly depend on the strength of the air jet. Therefore, the softness and viscoelastic properties of soft samples can

be determined by measuring the diameter and depth of dents for different strengths of the air jet and their changes with time. In the measurement of changes in the properties of viscoelastic samples with time, the developed test equipment has the following advantages: (1) The load to be applied to or removed from viscoelastic samples and its loading time can be arbitrarily set. (2) The loading process from the start of pressurization to the realization of the desired load and the unloading process from the end of pressurization to the realization of another desired load are almost instantaneous. (3) The state of deformation and the recovery of viscoelastic samples can be measured under conditions similar to those for loading or unloading using the air jet. (4) The damage and contamination of soft samples can be avoided owing to the noncontact nature of the method using compressed air.

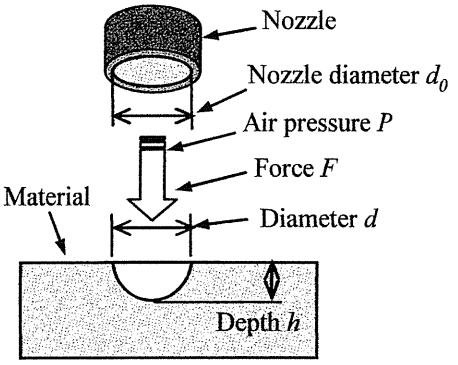

Fig.2 Measurement principle of surface texture

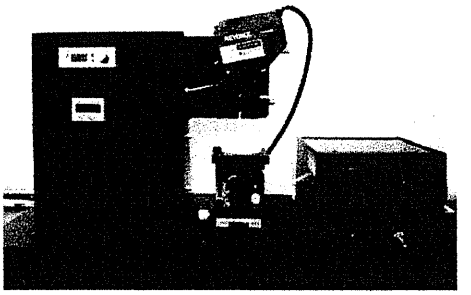

Fig.3 Summary of measuring equipment.

3.2 Noncontact-type test equipment using air jet

Figure 3 shows the noncontact-type functional test equipment, which comprises a compressor, an air tank for temporarily storing air, and a measurement unit. In the shape detection device, the depth and diameter of dents can be measured by irradiating visible light from a semiconductor laser with a large diameter onto a dent and collecting the reflected light using a two-dimensional charge-coupled device (CCD). The minimum measurable depth and dent diameter are 0.2 and 2.0 mm, respectively. A stable air jet was obtained when the nozzle diameter and ejection distance were 1.0 and 5.0 mm, respectively. The pressure explained in the experimental results section represents the pressure at the nozzle with the above dimensions, and the load was calculated from this pressure. The diameter and thickness of the

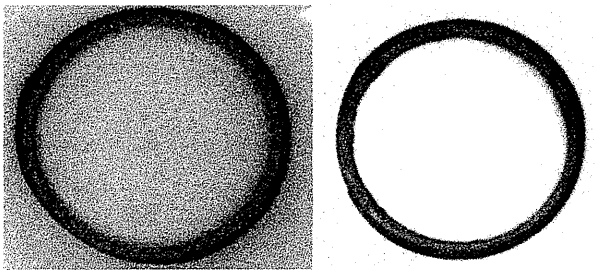

(a) Skin gel (b) Slime

Fig.4 Flexible materials for the experiment.

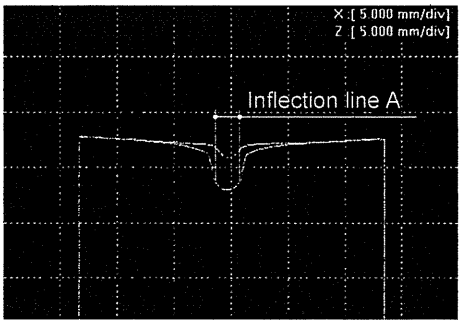

Fig.5 Cross section 2D shape which changed by the nozzle pressure.

soft samples used in this study were set to 50 and 20 mm, respectively, so as not to affect the measurement of the shape of dents. The samples used were human skin gel, slime, flan (or crème caramel), *kinu-dofu* (silken tofu) and *momen-dofu* (firm tofu).

4. Experimental Results

4.1 Viscoelastic properties for different loading times

Figure 5 shows the shape of the dent formed when the air jet was ejected onto the surface of the slime sample, obtained using the shape detection device. Figure 6 shows the creep and creep recovery curves for creep times of 5, 10, 15, and 20 s with the depth of the dent as the ordinate. Nonlinear delayed elastic deformation and viscous flow can be observed in the creep curves. The ratio of permanent deformation to elastic deformation decreased with increasing loading time. Therefore, it is considered that the elasticity of soft samples is related to the ratio of permanent deformation to elastic deformation caused by loading and that the elasticity of soft samples increases with decreasing loading time.

4.2 Viscoelastic properties of various soft samples

Measuring creep and creep recovery is an effective means of evaluating the depth of a dent formed on the surface of a soft sample when the surface is pressed or rubbed and how it recovers. Figure 7 shows the creep and creep recovery curves of samples of industrial materials (slime(green line) and human skin gel(purple line)) and processed food (flan(red line), silken tofu(light green line), and firm tofu(light blue line)) with the depth of the dent as the ordinate. In this experiment, the inner diameter of the nozzle was 1.0 mm, the ejection pressure was 20 kPa, the ejection time was 20 s, and the measurement time was 60 s. The depth of the dent up to a loading time of 7 s was greatest for the flan, indicating its greatest softness among all the samples. This was followed by slime, silken tofu, human skin gel, then firm tofu. After the loading time of 7 s, the depth of the dent on the slime exceeded that on the flan. This is considered to be because the instantaneous elastic deformation was dominant and the delayed elastic deformation and viscous flow were less dominant for the flan, whereas the viscous flow was dominant and the instantaneous and delayed elastic deformations were less dominant for the slime.

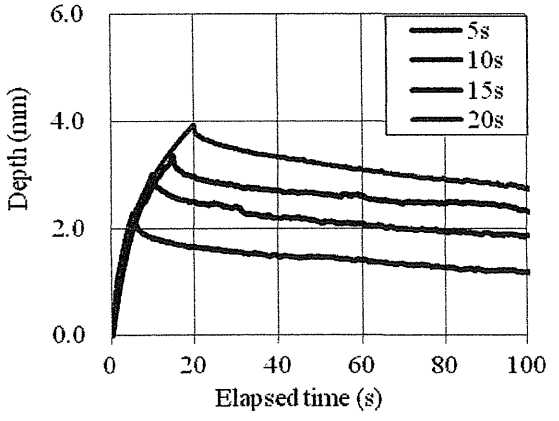

Fig.6 Variation of dents depth for creep time.

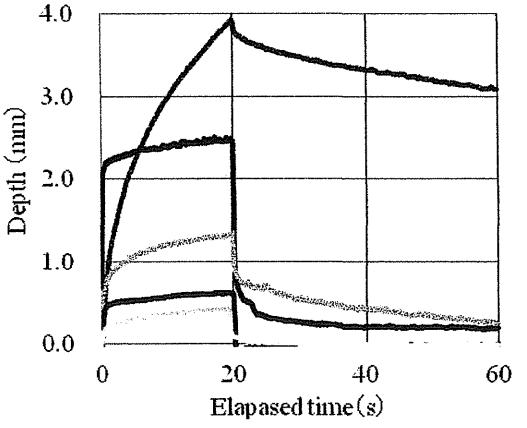

Fig.7 Elapsed time of dents depth which appeared on soft objects.

During the creep recovery for 40 s after the ejection had finished, the depth of the dent decreased most slowly with time for the slime. The depth of the dent was largest for the slime, which was followed by silken tofu, flan, then firm tofu. For the slime, instantaneous elastic

deformation hardly occurred and delayed elastic deformation was dominant. For the flan and silken tofu, three behaviors, i.e., instantaneous elastic deformation, delayed elastic deformation, and permanent deformation, were observed. For the human skin gel and firm tofu, the instantaneous elastic deformation was dominant during the creep recovery. From the above, the depth of the dent depends on the type of sample even under the same loading conditions, and therefore, soft samples can be compared and identified from differences in the depth of the dent; for example, slime is highly viscous, human skin gel is highly elastic, and tofu is viscoelastic.

4.3 Viscoelastic properties for various pressures of air jet

Figure 8 shows the changes in the depth of the dent with time when the human skin gel, slime, and silken tofu were exposed to an air jet. Five different pressures were applied and the inner diameter of the nozzle was 0.5 mm. To obtain the results for the human skin gel [Fig. 8(a)], ejection time was set to 30 s and pressure was changed in increments of 5 kPa between 40 and 60 kPa. Higher pressures were used for this sample than for the other samples because of the high elasticity of human skin gel. The depth of the dent was small at low pressures and large at high pressures. The dent was formed immediately after the start of loading and its depth sharply decreased immediately upon unloading, after which the human skin gel completely recovered within 5 s. This is because the rate of increase in dent depth was high when a load was suddenly applied, however, the viscosity was low and the creep recovery time was short when the loading time was short. Therefore, stress was considered to decrease in this time range. To obtain the results for the slime [Fig. 8(b)], which is a very soft material, ejection time was set to as short as 5 s and pressure was changed in increments of 5 kPa between 20 and 40 kPa. Comparatively low pressures were adopted to avoid breaking the surface of the slime with the air jet, which may disturb the measurement. It was found that the depth of the dent on the slime changed with time more slowly than that on the human skin gel at each pressure, showing that the viscous behavior was dominant with little elastic behavior. Although the depth of the dent exponentially decreased after unloading, the slime did not completely recover under any pressure even after a measurement time of 100 s, indicating its viscous behavior. The creep behavior of the silken tofu shown in Fig. 8(c) was intermediate between those of the human skin gel and slime. Elastic deformation was observed immediately after the start of loading, followed by viscoelastic behavior. Elastic deformation was also observed immediately after unloading, followed by a slow viscous recovery and plastic flow after a measurement time of 100 s. Waves with a short wavelength and a small amplitude were observed on each curve. This is considered to be because the final state of the tofu is affected by the generation of pores and the amounts of moisture, dietary fibers, and coagulants, and is nonuniform. For the silken tofu, ejection time was set to 20 s and pressure was changed in increments of 5 kPa between 20 and 40 kPa.

5. Discussion

5.1 Compliance in creep and creep recovery

The air jet ejected from the end of the nozzle causes soft samples to deform; the shape and dimensions of a dent formed on the sample surface depend on the distance from the end of the nozzle to the sample surface, i.e., ejection distance, even though nozzle pressure is constant. The load applied to the surface of the soft samples at each nozzle pressure when ejection distance was fixed at 5 mm was measured using a load meter in advance and used in the experiment. We measured the temporal changes in compliance, which is obtained by dividing the depth of the dent by the load. Compliance is given in mm/N, which is the inverse of spring constant, and represents the depth of the dent formed under a force of 1 N, i.e., the softness of a sample. Figure 9 shows the changes in compliance with time for the human skin